Int J Thermophys (2009) 30:1130–1143
DOI 10.1007/s10765-009-0620-4

Joule–Thomson Inversion in Vapor–Liquid–Solid Solution Systems

Dan Vladimir Nichita · Jerome Pauly · Jean-Luc Daridon

Received: 28 February 2009 / Accepted: 5 July 2009 / Published online: 22 July 2009

Abstract Solid phase precipitation can greatly affect thermal effects in isenthalpic expansions; wax precipitation may occur in natural hydrocarbon systems in the range of operating conditions, the wax appearance temperature being significantly higher (as high as 350 K) for hyperbaric fluids. Recently, methods for calculating the Joule–Thomson inversion curve (JTIC) for two-phase mixtures, and for three-phase vapor–liquid–multisolid systems have been proposed. In this study, an approach for calculating the JTIC for the vapor–liquid–solid solution systems is presented. The JTIC is located by tracking extrema and angular points of enthalpy departure variations versus pressure at isothermal conditions. The proposed method is applied to several complex synthetic and naturally occurring hydrocarbon systems. The JTIC can exhibit several distinct branches (which may lie within two- or three-phase regions or follow phase boundaries), multiple inversion temperatures at fixed pressure, as well as multiple inversion pressures at given temperature.

Keywords Equation of state · Inversion curve · Isenthalpic expansion · Joule–Thomson effect · Multiphase system · Solid precipitation · Wax

List of Symbols

a Attractive term in the cubic EoS, mixture
a_i Attractive term in the cubic EoS, component i
b Co-volume in the cubic EoS, mixture
b_i Co-volume in the cubic EoS, component i
f_i Fugacity, component i

D. V. Nichita (✉) · J. Pauly · J.-L. Daridon
Laboratoire des Fluides Complexes, CNRS UMR 5150, Université de Pau et des Pays de l'Adour, BP 1155, Pau Cedex 64013, France
e-mail: dnichita@univ-pau.fr

H	Enthalpy
h	Molar enthalpy
k_{ij}	Binary interaction parameter between components i and j
n_i	Feed mole number, component i
n_{ik}	Mole number of component i in phase k
n_k	Mole amount of phase k
nc	Number of components
np	Number of equilibrium phases
P	Pressure
R	Universal gas constant
T	Temperature
v	Molar volume
x_{ik}	Mole fraction of component i in phase k
Z	Compressibility factor

Greek Symbols

β	Proportionality coefficient
δ_1, δ_2	Constants in the cubic EoS
μ	Joule–Thomson coefficient

Subscripts

i	Component index
k	Phase index
V	Vapor
L	Liquid
S	Solid
t	Total

Superscripts

dep	Departure
E	Excess
ig	Ideal gas
tr	Transition
$*$	Apparent
LS	Liquid–solid transition
SS	Solid–solid transition

1 Introduction

Wax deposition is a major concern in the oil industry. In extracting oil from a reservoir and transporting it, wax precipitation may occur at any one of the stages along the flow, including in the formation near the well bore [1], within the well [2,3], and beyond the

well, in a conduit or pipeline, especially if the pipelines are multiphase, cold sub-sea lines. During depressurization, isentropic expansion may cause severe cooling due to the Joule–Thompson (JT) effect. In the formation near the well and at the well bottom, the crude oil temperature is normally, but not always, higher than its cloud point, avoiding wax precipitation. As the crude oil travels up the well, the temperature and pressure drop induces JT expansion which may cause further precipitation of wax.

Joule–Thomson expansion is a process in which the enthalpy of a fluid remains constant. As a consequence, the temperature will change when pressure drops, and this is generally referred to as the JT effect. Temperatures can either decrease or increase, depending on the initial pressure and temperature, final pressure, and composition of the fluid. The region where cooling takes place is separated from the region where heating takes place by the JT inversion curve (JTIC), which corresponds to the locus of points at which the JT coefficient $\mu_{\mathrm{JT}} = (\partial T/\partial P)_H$ equals zero.

Calculation of the JT coefficient and of the JTIC is a clear and well-documented matter for homogeneous fluids (pure components and mixtures), from both experimental [4,5] and theoretical points of view. The JTIC problem has been addressed using a variety of thermodynamic models, such as equations of state [6–13], and molecular simulation [14–18].

If the mixture splits into two or more phases, an apparent JT coefficient can be defined, which incorporates both JT effects and effects of phase distribution changes [19]. Calculations of the JTIC have been previously presented for two-phase vapor–liquid mixtures [19] and for three-phase vapor–liquid–multisolid systems [20].

Most experimental and simulation study on precipitation of heavy paraffins has been undertaken at atmospheric pressure for dead oils (i.e., oils at a sufficiently low pressure, which contain no more dissolved gas), fuels, and synthetic systems. Nevertheless, an investigation of paraffin precipitation cannot be dissociated from the pressure effect since the gases in the live oil (the oil which contains dissolved gas in solution that may be released from solution upon an expansion to surface conditions) can have a considerable influence on the wax appearance temperature (WAT), or cloud point, by decreasing it as much as 15 K between atmospheric and saturation conditions. The pressure effect has, thus, also to be well-described by a thermodynamic model in order to predict the risk of waxy solid deposits between bottom holes and surface facility conditions. Recently, the development of predictive local composition models for the description of wax formation in hydrocarbon fluids led to a highly successful tool for the simulation of wax formation in diesels, fuels, and dead and live oils [21–25].

This article is the second of a series dedicated to JTIC calculation for multiphase systems with solid phase precipitation. In the first one [20], we looked at model synthetic mixtures, several ternary mixtures (containing a light hydrocarbon, an intermediate solvent; and a heavy precipitating component), as well as a seven-component mixture designed to mimic a reservoir fluid were studied using a multisolid thermodynamic model [26] and a methodology based on isenthalpic phase equilibrium calculations [20,27]. In this study we propose a method for calculation of apparent JTIC, suitable for multiphase complex hydrocarbon systems involving solid phase (which is described as a solid solution) precipitation. The thermodynamic model used to describe the multiphase behavior of such mixtures is based on the predictive approach developed by

Pauly et al. [21]. The enthalpy-based method does not require isenthalpic flash calculations; the location of the JTIC is found by tracking the minima and angular points of enthalpy departure variation with pressure at isothermal conditions.

The article is structured along the following lines: first the JTIC for multiphase systems is described, then the JTIC construction procedure and the thermodynamic model are presented, and finally the proposed method is applied to several complex hydrocarbon mixtures (two synthetic systems and a North Sea gas condensate), before drawing the conclusions.

2 JTIC for Multiphase Systems

As discussed in [19], an apparent JT coefficient can be defined for multiphase (*np* phases) multicomponent (*nc* components) mixtures of composition $\boldsymbol{n} = (n_1, \ldots, n_{nc})^T$, as

$$\mu^* = \left(\frac{\partial T}{\partial P}\right)_{H_t,\boldsymbol{n}} \tag{1}$$

where the derivation is carried out with respect to the total enthalpy, $H_t = \sum_{k=1}^{np} H_k$, and to the feed mole numbers n_i $(i = 1, nc)$.

An equivalent form of the JTIC equation ($\mu^* = 0$) is [19]

$$\left(\frac{\partial H_t}{\partial P}\right)_{T,\boldsymbol{n}} = 0 \tag{2}$$

It is incorrect to use the feed composition to calculate the JTIC inside the phase envelope, since the thermodynamically stable state corresponding to a minimum Gibbs energy corresponds to a phase split. The JTIC can have several distinct branches, located in the single-phase region and either within the two- and three-phase regions, or on the phase boundaries, and several inversion temperatures (pressures) can be recorded at given pressures (temperatures) [19,20].

Several (volume-based and enthalpy-based) methods for JTIC calculation have been proposed by Nichita and Leibovici [19] for two-phase vapor–liquid systems. The volume-based method cannot be applied to fluid–solid equilibria; thus, an enthalpy-based approach should be adopted if solid phase equilibrium is involved. In a previous study of the JTIC in multiphase systems [20], the JTIC was constructed by performing isenthalpic flash calculations and tracking sign changes of partial derivatives $(\partial T/\partial P)_{H_t,\boldsymbol{n}}$ or $(\partial H_t/\partial P)_{T_t,\,\boldsymbol{n}}$.

In this study, a different enthalpy-based approach is used, i.e., an alternative form of the JTIC equation is used [19]:

$$\left(\frac{\partial H^{\mathrm{dep}}}{\partial P}\right)_{T,\boldsymbol{n}} = 0 \tag{3}$$

where H^{dep} is the enthalpy departure of the multiphase system, i.e., the sum of phase enthalpy departures. Equation 3 gives minima of H^{dep}, which corresponds to the JTIC branches located within the two- or three-phase regions. The JTIC also has several branches which follow the phase boundaries [20]; at phase boundaries, the variation of the enthalpy departure with pressure at a given temperature exhibits angular points, corresponding to discontinuities (thresholds from positive/negative to negative/positive values) of the apparent JT coefficient.

3 Phase Envelopes and the JTIC Construction

Liquid–vapor phase boundaries are constructed using an efficient method for mixtures with many components [28]. Critical points are calculated [29,30] using the Heidemann and Khalil [31] criticality criteria. Solid phase boundaries (liquid–solid or vapor–solid, vapor–liquid/vapor–liquid–solid, and vapor–liquid–solid/liquid–solid) are located using a multiphase vapor–liquid–solid flash algorithm by minimization of the Gibbs free energy, and by a tangent plane distance function minimization for phase stability analysis [32,33].

The single-phase JTIC is constructed, and the portion of the curve situated within the phase envelope is discarded [13]; then the JTIC in the two- and three-phase regions is constructed using the enthalpy-based approach as proposed by Nichita and Leibovici [19]. For a given isotherm, flash calculations are performed covering the appropriate pressure interval, and the intersection(s) of the isotherm(s) with the JTIC is (are) found by tracking the minima and angular points (with change in slope sign) of the enthalpy departure variation versus pressure. An isotherm can intersect the JTIC several (up to three) times, as will be shown in the Sect. 5.

The approach proposed here is not model-dependent. For any thermodynamic model, one needs only to provide the specific enthalpy departure $h_k^{\mathrm{dep}}(P, T, \boldsymbol{x_k})$ and component fugacity $f_{ik}(P, T, \boldsymbol{x_k})$; $k = \mathrm{L}, \mathrm{V}, \mathrm{S}$ functions (where $\boldsymbol{x_k} = (x_{1k}, \ldots, x_{nc,k})^T$ is the vector of mole fractions in the phase "k"). As will be shown in the next section, a calculation of the ideal-gas enthalpy is not required.

4 Thermodynamic Model

The thermodynamic model for wax precipitation of Pauly et al. [21] is used. Next, fugacity and enthalpy calculations are briefly presented.

Component fugacities in the liquid and vapor phases are calculated from the two-parameter Peng–Robinson (PR) cubic equation of state (EoS) [34]. The fugacity of a component present in the solid phase is calculated from

$$f_{i\mathrm{S}}(P, T, \boldsymbol{x_S}) = x_{i\mathrm{S}}\gamma_{i\mathrm{S}}(\boldsymbol{x_S})[f_{i\mathrm{L}_0}(P_0)]^{1-\beta}[f_{i\mathrm{L}_0}(P)]^{\beta} \exp\left[-\frac{\Delta H_i^{\mathrm{SL}_0}}{RT}\left(1-\frac{T}{T_i^{\mathrm{SL}_0}}\right)\right.$$
$$\left.-\frac{\Delta H_i^{\mathrm{tr}_0}}{RT}\left(1-\frac{T}{T_i^{\mathrm{tr}_0}}\right)\right] \tag{4}$$

where β is a proportionality coefficient, assumed to be pressure-independent ($\beta = 0.9$ [21]), and γ_{iS} is the solid activity coefficient, calculated from the predictive Wilson equation [35]; the interaction between molecule chain ends is taken into account by an adjustable bending parameter ξ [23], which is used to match the wax appearance temperature at low pressures.

The total enthalpy can be written as the sum of two contributions, the ideal-gas enthalpy and the enthalpy departure,

$$H_t = H^{ig} + H^{dep} \tag{5}$$

The total enthalpy of a multiphase system with np equilibrium phases is the sum of phase enthalpies,

$$H_t = \sum_{k=1}^{np} H_k = \sum_{k=1}^{np} n_k h_k \tag{6}$$

where n_k ($k = V, L, S$) are the mole amounts of phase "k", and phase enthalpies are the sum of ideal-gas enthalpy and enthalpy departure contributions

$$H_k = H_k^{ig} + H_k^{dep} \tag{7}$$

The total enthalpy can be also written as

$$H_t = H^{ig}(\boldsymbol{n}) + \sum_{k=1}^{np} H_k^{dep}(\boldsymbol{n_k}) \tag{8}$$

where $\boldsymbol{n_k} = (n_{1k}, \ldots, n_{nc,k})^T$ is the vector of mole numbers in the phase "k")

The ideal-gas enthalpy does not depend on pressure directly or via phase mole fractions [19] (thus, $(\partial H^{ig}/\partial P)_T = 0$), and its calculation is necessary only if the total enthalpy is required (as for isenthalpic flash calculations in [20]); in this study, we need only the partial derivative $(\partial H^{dep}/\partial P)_{T,\boldsymbol{n}} = (\partial H_t/\partial P)_{T,\boldsymbol{n}}$; therefore, only the enthalpy departure is calculated.

The enthalpy departure of the multiphase system is

$$H^{dep} = \sum_{k=1}^{np} H_k^{dep}(\boldsymbol{n_k}) \tag{9}$$

Enthalpy departures of the fluid phases are calculated directly from the EoS. For the PR two-parameter cubic EoS [34], the expression for the molar enthalpy departure is

$$h_k^{dep}(P, T, \boldsymbol{x_k}) = RT(Z_k - 1) - \frac{1}{2\sqrt{2}b_k RT}\left[a_k - T\frac{da_k}{dT}\right]\ln\left[\frac{v_k + (1+\sqrt{2})b_k}{v_k + (1-\sqrt{2})b_k}\right]; \quad k = \text{L,V} \tag{10}$$

where $a_k = \sum_i \sum_j x_{ki} x_{kj} \sqrt{a_i} \sqrt{a_j} (1 - k_{ij})$ and $b_k = \sum_i x_{ki} b_i$, and the phase enthalpy is $H_k^{\text{dep}} = n_k h_k^{\text{dep}}$.

The enthalpy of a component in the solid phase is given by

$$H_{i\text{S}}(T, P) = (1 - \beta) H_{i\text{L}_0}(T, P_0) + \beta H_{i\text{L}_0}(T, P) + \Delta H_i^{\text{LS}}(T_i^{\text{LS}}, P_0) + \Delta H_i^{\text{SS}}(T_i^{\text{SS}}, P_0) \quad (11)$$

The derivation of Eq. 11 can be found in [20].

The enthalpy of the solid phase is

$$H_{\text{S}} = \sum_{i=1}^{nc} x_{i\text{S}} H_{i\text{S}} + H_{\text{S}}^{\text{E}} \quad (12)$$

where the excess enthalpy is $H_{\text{S}}^{\text{E}} = G_{\text{S}}^{\text{E}} - T \left(\frac{\partial G_{\text{S}}^{\text{E}}}{\partial T} \right)_{P, \boldsymbol{n}_{\text{S}}}$, and the partial derivative can be evaluated numerically.

In Eq. 11, $H_{i\text{L}_0} = n_{i\text{S}}(h_i^{\text{ig}} + h_{i\text{L}_0}^{\text{dep}})$; taking into account that the ideal terms go to the first term in Eq. 7, the solid phase enthalpy departure can be written as

$$H_{\text{S}}^{\text{dep}} = \sum_{i=1}^{nc} x_{i\text{S}} [\beta H_{i\text{L}_0}^{\text{dep}}(T, P) + \Delta H_i^{\text{LS}}(T_i^{\text{LS}}, P_0) + \Delta H_i^{\text{SS}}(T_i^{\text{SS}}, P_0)] + H^{\text{E}} \quad (13)$$

and the enthalpy departure of the multiphase system is finally calculated from Eqs. 9, 10, and 13.

5 Results

This section presents the results of JTIC calculation for three selected examples (two synthetic hydrocarbon mixtures and a reservoir fluid). All the examples were addressed previously in a different context in [36], and mixture characterization used there is adopted in this study. Component properties (critical temperature, critical pressure, and acentric factor) are taken from Reid et al. [37] (light hydrocarbon and non-hydrocarbon components) and from Twu [38] (heavy hydrocarbon components). Fusion and transition properties of heavy normal alkanes are taken from Pauly et al. [21].

5.1 Mixture B

The first example is a 15-component synthetic heavy paraffin mixture (Mixture B of Daridon et al. [39]) containing methane, an intermediate solvent (normal-decane), and heavy paraffins (from nC_{18} to nC_{30}). Heavy component mole fractions follow approximately an exponential decay with carbon number. Only the binary interaction

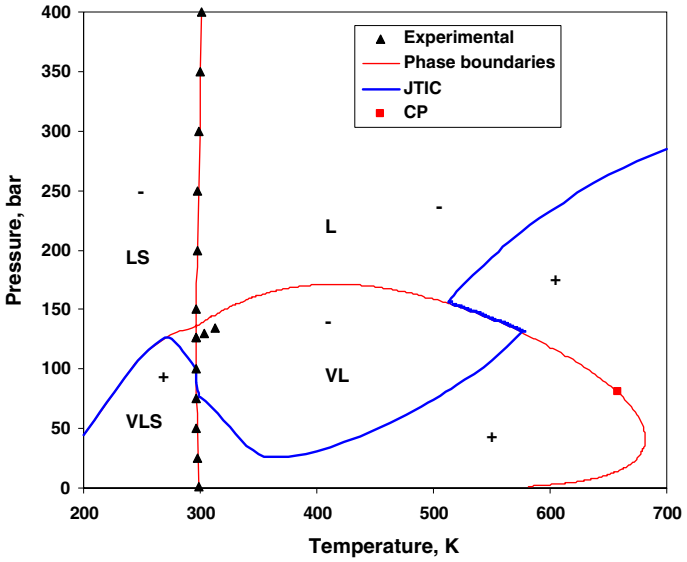

Fig. 1 Phase envelope and JTIC for mixture B

parameters (BIPs) of methane with heavy components are non-zero. The wax appearance temperature (WAT) at $P = 1$ bar is matched by adjusting the Wilson parameter ($\xi = -0.043$).

The phase envelope (calculated and experimental points) and the JTIC are plotted in Fig. 1 (the $+/-$ signs denote regions where heating or cooling occur upon isenthalpic expansions). The calculated [29] critical point is at $T = 657.7$ K and $P = 82.6$ bar. The JTIC has six distinct branches: in the single-phase liquid region, on the bubble point locus, within the two-phase liquid–vapor region, on the cloud point locus, within the three-phase vapor–liquid–solid region, and on the three-phase bubble point. There are up to four inversion temperatures at a given pressure, and up to three inversion pressures at a given temperature. The results are qualitatively similar to what was predicted for ternary mixtures [20].

5.2 North Sea Gas Condensate

The second example is a North Sea HP-HT reservoir fluid (mixture GC-B from Daridon et al. [40]). The initial reservoir pressure is 1100 bar and the reservoir temperature is 459 K. Mixture composition is characterized by 40 components, among which 25 components (paraffins from C_{11} to C_{35}) precipitate in the solid phase. All required elements for the fluid description can be found in [36,40].

Figure 2 presents the phase envelope (calculated and experimental points) and the calculated JTIC. The critical point is located at $T = 378.6$ K and $P = 327.4$ bar. It is interesting to note that the calculated (there are no experimental data available in the low temperature region) three-phase bubble point exhibits a shape similar to that of the two-phase bubble point (open shaped, or "S"-shaped).

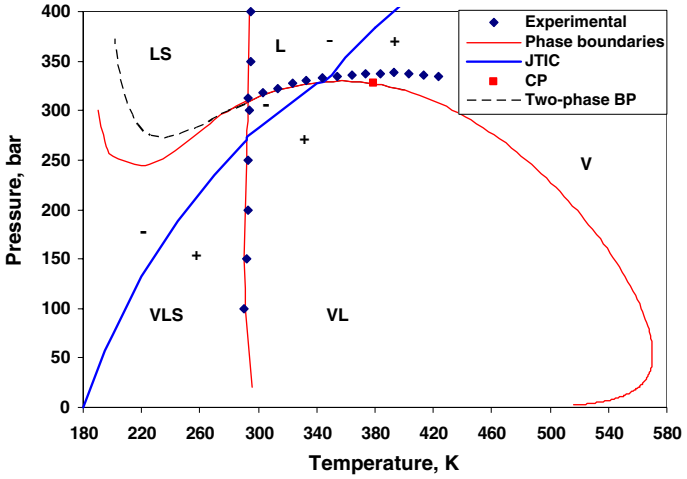

Fig. 2 Phase envelope and JTIC for a North Sea gas condensate

The JTIC exhibits five distinct branches: in the single-phase liquid region, on the bubble-point locus, inside the two-phase liquid–vapor region, on the cloud-point locus, and on the three-phase bubble point. There are up to four inversion temperatures at a given pressure, and up to three inversion pressures at a given temperature. There are no more than two inversion temperatures (pressures) at a given pressure (temperature). Note that for this mixture there is no branch of JTIC in the three-phase VLS region; the JTIC follows entirely the three-phase bubble-point locus.

Details of Fig. 2 are given in Fig. 3a (JTIC around the WAT locus) and in Fig. 3b (JTIC around bubble point locus), showing small thresholds of the JTIC. Even though the influence of phase split on JTIC seems very small for this system, one can note that the difference between the actual JTIC and the one that could be (incorrectly) calculated for the feed composition is, for instance, about 100 bar at $T = 290$ K.

On the other hand, concerning the little influence of solid phase precipitation on the JTIC, it should be noticed that, at a temperature just below the WAT, the calculated solid phase mole fractions of this mixture are about two orders of magnitude lower than those for Mixture B, and about one order of magnitude lower than those for mixture C_1/M8 (the results of phase distribution calculations for all three mixtures are reported in [36]).

5.3 Synthetic Mixture C_1/M8

The last example is a synthetic mixture of about 99 mol% methane and 10 heavy paraffins (ranging from nC_{13} to nC_{22}). Mixture composition and non-zero binary interaction parameters (BIPs) of methane with heavy components can be found in [36].

The phase envelope (calculated and experimental points) and the JTIC are drawn in Fig. 4. This mixture has no critical point (only dew points). A remarkable difference, from both qualitative and quantitative (hundreds of bars at a given temperature) points

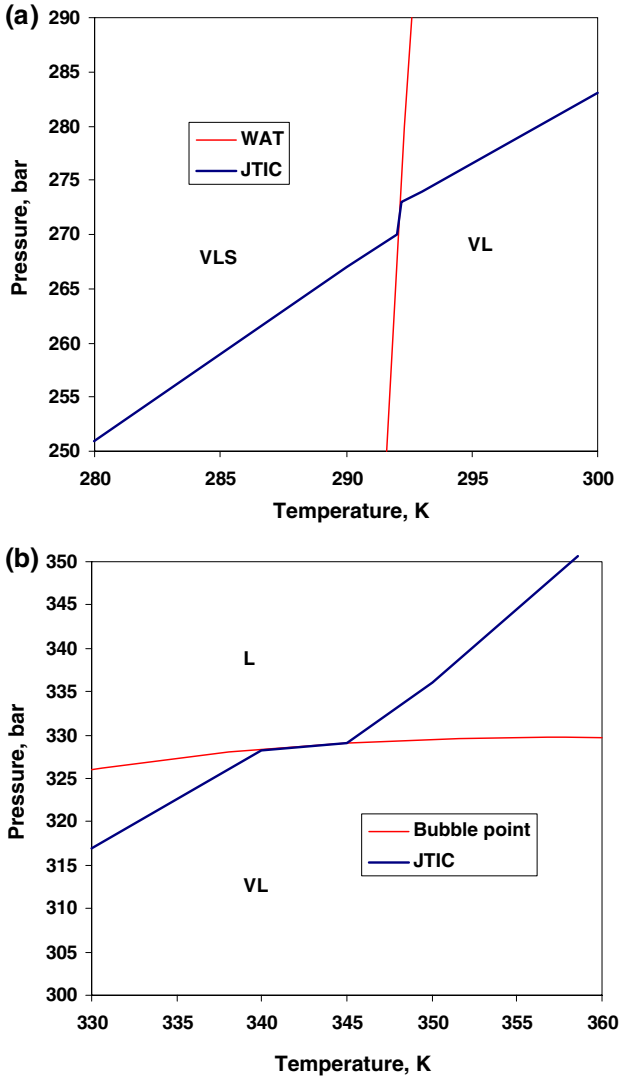

Fig. 3 Phase envelope and JTIC for a North Sea gas condensate (detail)

of view, can be noted between the three-phase dew point (which is the actual phase boundary) and the two-phase dew point (calculated with a two-phase vapor–liquid package, dashed line in Fig. 4). Retrograde behavior of both liquid and solid phases occurs below the three-phase dew point [41] upon isothermal expansion.

For this mixture, the JTIC has seven distinct branches: in the single-phase vapor region, on the dew-point locus, within the two-phase vapor–liquid region, on the cloud-point locus, within the three-phase vapor–liquid–solid region, on the three-phase dew-point locus, and within the two-phase vapor–solid region. There are up to

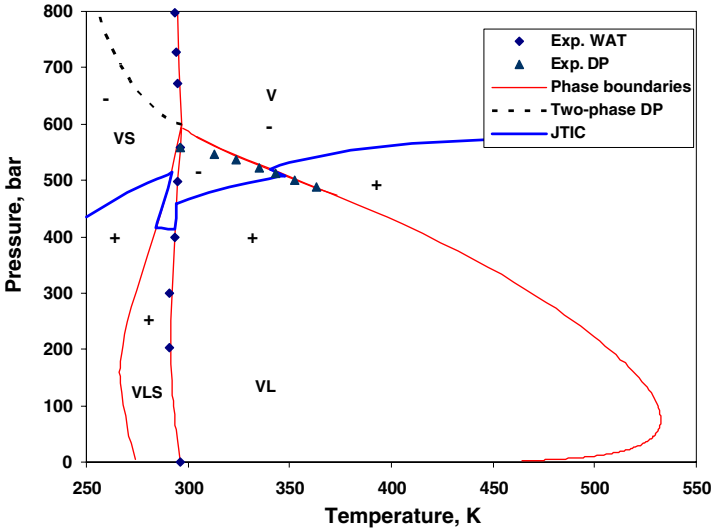

Fig. 4 Phase envelope and JTIC for C_1/M8 mixture

three inversion pressures at a given temperature, and up to four inversion temperatures at a given pressure.

The variations of the dimensionless enthalpy departure (H^{dep}/RT) versus pressure at different temperatures are plotted in Figs. 5a–e (dashed lines mark the three-phase dew points). For $T < 284\,\text{K}$, there is a single inversion (at the three-phase dew point). For $284\,\text{K} < T < 292\,\text{K}$, there are three inversion pressures (as shown in Figs. 5a to c for three different temperatures); the minimum at the lower pressure (with H^{dep} decreasing with temperature) corresponds to the inversion in the three-phase vapor–liquid–solid region, the angular point to the inversion at the three-phase dew point, and the minimum at higher pressure (with H^{dep} increasing with temperature) to the inversion in the two-phase vapor–solid region.

At a temperature around $T = 292\,\text{K}$, the third minimum (at higher pressure) in $H^{\text{dep}}(P)$ becomes an angular point (see Fig. 5d). There are only two inversion pressures at the temperature T^* (the intersection between the three-phase dew-point locus and the JTIC branch in the vapor–solid region) for which $\lim_{\substack{T\to T^* \\ T<T^*}} \left(\frac{\partial H_t}{\partial P}\right)_{T,\boldsymbol{n}} > 0$ and $\lim_{\substack{T\to T^* \\ T>T^*}} \left(\frac{\partial H_t}{\partial P}\right)_{T,\boldsymbol{n}} = 0$.

For $T > 292\,\text{K}$, the mixture exhibits a single inversion pressure (in the single-phase vapor region, at the two-phase dew-point, and within the two-phase liquid–vapor region), except in a small temperature window where there are three inversion pressures at a given temperature). Figure 5e shows the inversion in the vapor–liquid–solid region at $T = 294\,\text{K}$. Note that an angular point replaced the three-phase minimum, and that at the three-phase dew point, the left and right side slopes of the angular point have the same sign, i.e., $(\partial H_t/\partial P)_{T,\boldsymbol{n}} > 0$; thus, there is no inversion at this pressure.

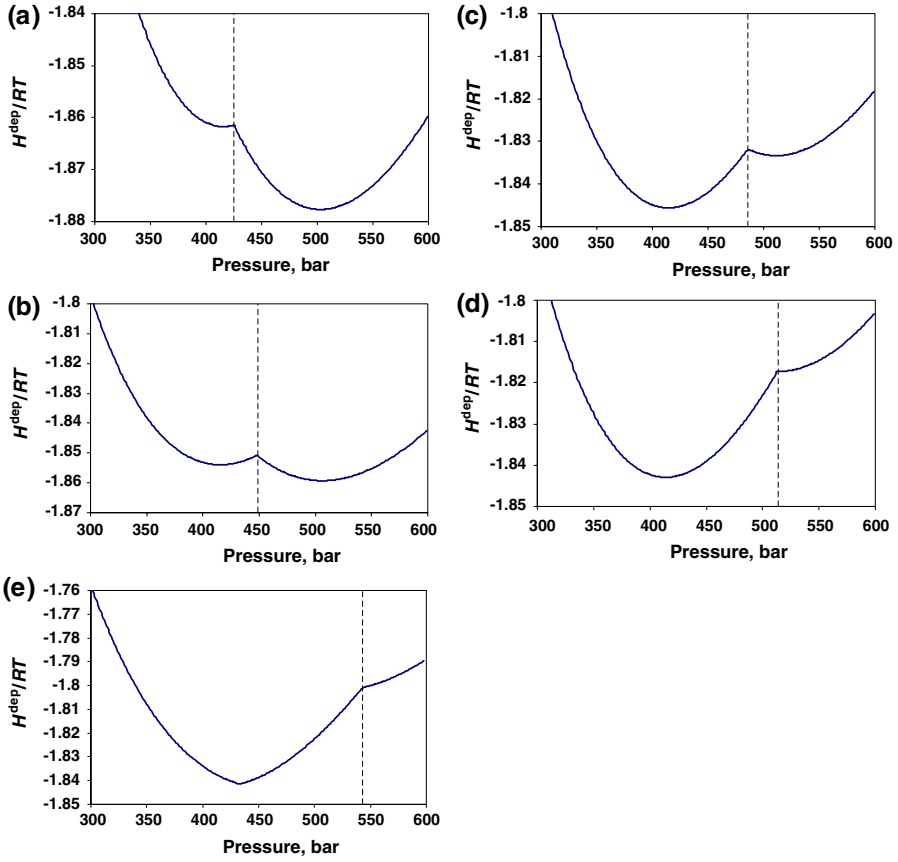

Fig. 5 Enthalpy departure variation for C_1/M8 mixture: (**a**) $T = 285$ K isotherm, (**b**) $T = 287$ K isotherm, (**c**) $T = 290$ K isotherm, and (**d**) $T = 292$ K isotherm, and (**e**) $T = 294$ K isotherm

6 Conclusions

Solid-phase precipitation may occur in natural hydrocarbon systems in the range of operating conditions normally encountered in the oil industry, and may affect the thermal effects of isenthalpic expansions. In this article, the apparent JTIC is calculated for complex hydrocarbon mixtures exhibiting solid waxy phase precipitation using a suitable vapor–liquid–solid solution thermodynamic model. For the JTIC construction, an enthalpy-based approach is adopted. The location of the JTIC is found by tracking minima (located within the two- and three-phase regions) or angular points (with change of the slopes' sign, located at phase boundaries) of enthalpy departure variation with pressure at a constant temperature. The proposed method is applied to several complex synthetic and naturally occurring hydrocarbon systems, which exhibit various phase envelopes and JTIC shapes. The JTIC may have several distinct branches (up to seven in our examples), including within two- and three-phase regions; the JTIC

shows multiple inversion temperatures at a given pressure (up to four), and multiple inversion pressures at a given temperature (up to three).

The effect of solid waxy phase precipitation on thermal effects in complex hydrocarbon mixtures seems to be quantitatively less pronounced and qualitatively less diverse than that calculated previously for model ternary systems; in other words, these effects are controlled rather by system asymmetry than by its complexity, and the presence in the mixture of a continuum containing components of homologous series tends to attenuate thermal effects.

Acknowledgment We thank Prof. Alain Graciaa (Université de Pau et des Pays de l'Adour) for his support.

References

1. K.J. Leontaritis, World Oil **220**, 87 (1999)
2. C. Jones, The use of bottomhole temperature variations in production testing. Paper SPE 18381, presented at the SPE European Petroleum Conference, London, 1988, pp. 423–431
3. A.C. Baker, M. Price, Modelling the performance of high-pressure high-temperature wells. Paper SPE 20903, presented at the SPE European Petroleum Conference, The Hague, 1990
4. D. Bessières, T. Lafitte, J.-L. Daridon, S. Randzio, Thermochim. Acta **428**, 25 (2005)
5. D. Bessières, S.L. Randzio, M.M. Pineiro, T. Lafitte, J.L. Daridon, J. Phys. Chem. B **110**, 5659 (2006)
6. K. Juris, L.A. Wenzel, AIChE J. **18**, 684 (1972)
7. G.W. Dilay, R.A. Heidemann, Ind. Eng. Chem. Fundam. **25**, 152 (1986)
8. D. Geana, V. Feroiu, Fluid Phase Equilib. **77**, 121 (1992)
9. J. Wisniak, H. Avraham, Thermochim. Acta **286**, 33 (1996)
10. J. Wisniak, H. Avraham, Ind. Eng. Chem. Res. **35**, 844 (1996)
11. W.G. Kortekaas, C.J. Peters, J. de Swaan Arons, Fluid Phase Equilib. **139**, 205 (1997)
12. N.S. Matin, B. Haghighi, Fluid Phase Equilib. **175**, 273 (2000)
13. C.F. Leibovici, D.V. Nichita, Chem. Eng. Commun. **194**, 648 (2007)
14. C.M. Colina, E.A. Muller, Int. J. Thermophys. **20**, 229 (1999)
15. C.M. Colina, L.F. Turrens, K.E. Gubbins, C. Olivera-Fuentes, L.F. Vega, Ind. Eng. Chem. Res. **41**, 1069 (2002)
16. C.M. Colina, M. Lisal, F.R. Siperstein, K.E. Gubbins, Fluid Phase Equilib. **202**, 253 (2002)
17. M.H. Lagache, P. Ungerer, A. Boutin, Fluid Phase Equilib. **220**, 211 (2004)
18. J. Vrabec, G.K. Kedia, H. Hasse, Cryogenics **45**, 253 (2005)
19. D.V. Nichita, C.F. Leibovici, Fluid Phase Equilib. **246**, 167 (2006)
20. D.V. Nichita, D. Bessieres, J.L. Daridon, Energy Fuels **22**, 4012 (2008)
21. J. Pauly, J.L. Daridon, J.A.P. Coutinho, N. Lindeloff, S.I. Andersen, Fluid Phase Equilib. **167**, 145 (2000)
22. J.A.P. Coutinho, J.L. Daridon, Energy Fuels **15**, 1454 (2001)
23. J.M. Sansot, J. Pauly, J.L. Daridon, J.A.P. Coutinho, AIChE J. **51**, 2089 (2005)
24. J.A.P. Coutinho, C. Gonçalves, I.M. Marrucho, J. Pauly, J.L. Daridon, Fluid Phase Equilib. **233**, 28 (2005)
25. J.A.P. Coutinho, F. Mirante, J. Pauly, Fluid Phase Equilib. **247**, 8 (2006)
26. C. Lira-Galeana, A. Firoozabadi, J.M. Prausnitz, AIChE J. **42**, 239 (1996)
27. M.L. Michelsen, Fluid Phase Equilib. **33**, 13 (1987)
28. D.V. Nichita, Energy Fuels **22**, 488 (2008)
29. D.V. Nichita, Fluid Phase Equilib. **228–229**, 223 (2005)
30. D.V. Nichita, AIChE J. **52**, 1220 (2006)
31. R.A. Heidemann, A.M. Khalil, AIChE J. **26**, 769 (1980)
32. D.V. Nichita, S. Gomez, E. Luna, Fluid Phase Equilib. **194–197**, 411 (2002)
33. D.V. Nichita, S. Gomez, E. Luna, Comput. Chem. Eng. **26**, 1703 (2002)
34. D.Y. Peng, D.B. Robinson, Ind. Eng. Chem. Fundam. **15**, 59 (1976)
35. G.M. Wilson, J. Am. Chem. Soc. **86**, 127 (1964)

36. D.V. Nichita, J. Pauly, F. Montel, J.L. Daridon, Energy Fuels **22**, 775 (2008)
37. R.C. Reid, J.M. Prausnitz, B.E. Poling, *The Properties of Gases and Liquids*, 4th edn. (McGraw-Hill, New York, 1987)
38. C.E. Twu, Fluid Phase Equilib. **11**, 65 (1983)
39. J.L. Daridon, P. Xans, F. Montel, Fluid Phase Equilib. **117**, 241 (1996)
40. J.L. Daridon, J. Pauly, J.A.P. Coutinho, F. Montel, Energy Fuels **15**, 730 (2001)
41. D.V. Nichita, L. Goual, A. Firoozabadi, SPE Prod. Facil. **16**, 250 (2001)